

Dynamic Remanent Vortices in Superfluid $^3\text{He-B}$

R.E. Solntsev[†], R. de Graaf[†], V.B. Eltsov^{†‡}, R. Hänninen[†],
and M. Krusius[†]

[†] *Low Temperature Laboratory, Helsinki University of Technology, Finland*

[‡] *Kapitza Institute for Physical Problems, Kosygina 2, 119334 Moscow, Russia*

We investigate the decay of vortices in a rotating cylindrical sample of $^3\text{He-B}$, after rotation has been stopped. With decreasing temperature vortex annihilation slows down as the damping in vortex motion, the mutual friction dissipation $\alpha(T)$, decreases almost exponentially. Remanent vortices then survive for increasingly long periods, while they move towards annihilation in zero applied flow. After a waiting period Δt at zero flow, rotation is reapplied and the remnants evolve to rectilinear vortices. By counting these lines, we measure at temperatures above the transition to turbulence $\sim 0.6T_c$ the number of remnants as a function of $\alpha(T)$ and Δt . At temperatures below the transition to turbulence $T \lesssim 0.55T_c$, remnants expanding in applied flow become unstable and generate in a turbulent burst the equilibrium number of vortices. Here we measure the onset temperature T_{on} of turbulence as a function of Δt , applied flow velocity $\mathbf{v} = \mathbf{v}_n - \mathbf{v}_s$, and length of sample L .

PACS numbers: 67.40.Vs, 47.32.Cc.

In superfluid $^3\text{He-B}$ the length scale of the vortex core radius is the superfluid coherence length $\xi(T) = \xi(0)(1 - T/T_c)^{-1/2}$, with $\xi(0) = 12 - 65$ nm for pressures $P = 34 - 0$ bar. Apparently this is large enough compared to the typical surface roughness of our fused quartz sample cylinder that it has not been possible to measure surface pinning or surface friction. A sensitive test is to check for vortex formation when flow is applied, to find out whether vortices have remained pinned at surface traps for indefinitely long waiting periods Δt in zero applied flow. If Δt is long enough, all remnants have annihilated, unless they become permanently pinned. At mK temperatures the energy barriers associated with such pinning traps are typically large compared to thermal energies and once loaded, a trap remains occupied as long as the flow velocity v is kept at sufficiently low level. To release a remnant from the trap, the required applied flow velocity is $v_c \approx 0.8\kappa/(2\pi r_o)$, if the remnant is modeled as a half circle of radius r_o

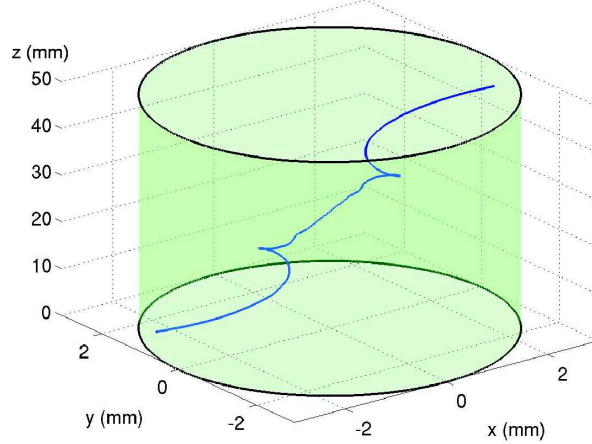


Fig. 1. A single remanent vortex in an ideal cylinder (with no pinning or surface friction) at zero applied flow in ${}^3\text{He-B}$ ($0.40 T_c$, 29 bar). Both ends of the vortex move slowly in spiral motion around the cylindrical wall in the image flow field created by the vortex itself. This snapshot shows the configuration after 1.3 h of motion towards final annihilation which takes 2.3 h. The vortex was initially straight but tilted, with its ends at $(-1,0,0)$ and $(1,0,50)$ on the two flat end plates of the cylinder, which is 50 mm long and 3 mm in radius.

attached at both ends to the cylindrical wall.¹

This measurement is straightforward, but it involves three complications: (i) Remnants can exist on different length scales. The length scale determines the flow velocity at which a particular remnant is inflated out of the pinning trap. (ii) In the presence of only a few isolated pinning traps remanence has stochastic nature since during random annihilation a particular pinning site may or may not become loaded with a remnant. (iii) The dynamical behavior of vortices changes with temperature because of the strong temperature dependence of mutual friction dissipation $\alpha(T, P)$.² At high temperatures vortex motion is rapid and number conserving. When rotation is here suddenly stopped from an equilibrium vortex state at $\Omega(t=0)$, the decay of rectilinear vortices is of the form³ $N(t) \propto (1 + t/\tau)^{-1}$, with a decay time $\tau = [2\alpha\Omega(0)]^{-1}$.

In contrast, at low temperatures the motion of an isolated vortex at zero applied flow becomes sluggish, as known from ${}^4\text{He-II}$. Below $0.5 T_c$ the motion of the last vortex towards total annihilation may require hours, as seen in the numerically calculated⁴ example in Fig. 1. In this situation it becomes experimentally difficult to distinguish between *pinned remnants* and

Dynamic remanent vortices in $^3\text{He-B}$

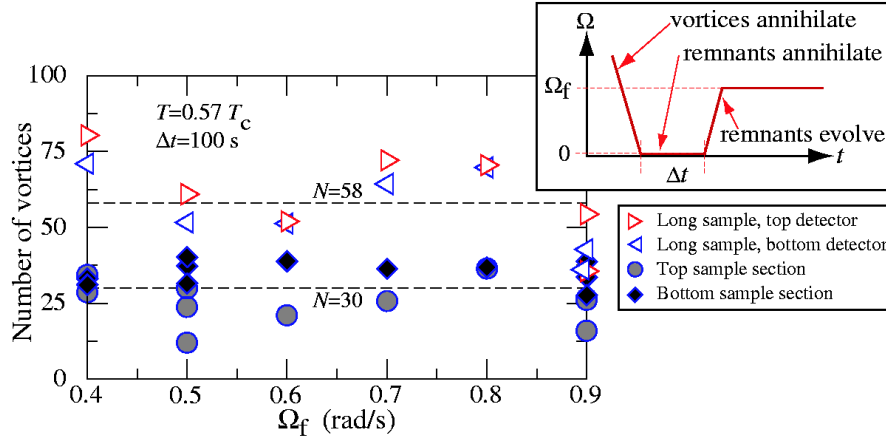


Fig. 2. Number of remnants \mathcal{N} after a waiting period $\Delta t = (100 \pm 5)$ s, measured as a function of Ω_f . The average for the A-phase separated top and bottom sections is 30 and for the long sample 58. (*Insert*) Measuring procedure and rotation drive.

dynamic remnants.

Experimental setup: We measure with non-invasive NMR techniques the number of vortex lines at 29.0 bar pressure in a sample cylinder with radius $R = 3$ mm and length $L = 110$ mm. The axis of the cylinder is tilted by an angle of 0.64° from the rotation axis. NMR detection coils are located close to both ends of the sample.⁵ The sample can also be studied in a second configuration: By sweeping up a magnetic barrier field $H_b > H_{AB}(T, P)$ over the central section of the long sample, a layer of $^3\text{He-A}$ is created. It divides the cylinder in two separated $^3\text{He-B}$ sections which can be studied independently, because the A phase layer acts as a barrier⁵ for vortices. With a fixed current ($I_b = 6.0$ A) in the barrier magnet, the B-phase sections have the lengths $L_t = 44$ mm (41 mm) for the top and $L_b = 54$ mm (51 mm) for the bottom sections at $0.57 T_c$ ($0.70 T_c$). By rotating the sample cylinder with angular velocity Ω , the maximum flow velocity is reached at the cylindrical wall, $v(\Omega, N) = \Omega R - \kappa N / (2\pi R)$, where N is the number of rectilinear vortex lines in a central vortex cluster. N is determined by comparing the NMR line shape to one measured with a known number of vortices (taking into account the tilt angle between axes).¹

Measuring procedure: The measurement is started from a state with large N at $\Omega \gtrsim 1.7$ rad/s which is decelerated at 0.02 rad/s² to zero rotation and kept there for a waiting period Δt . Rotation is then increased (in the same direction) at 0.01 rad/s² to Ω_f where it is kept constant (see insert in Fig. 2). The NMR line shape measured at Ω_f , after all transients have decayed, is compared to a calibration with a known number of rectilinear

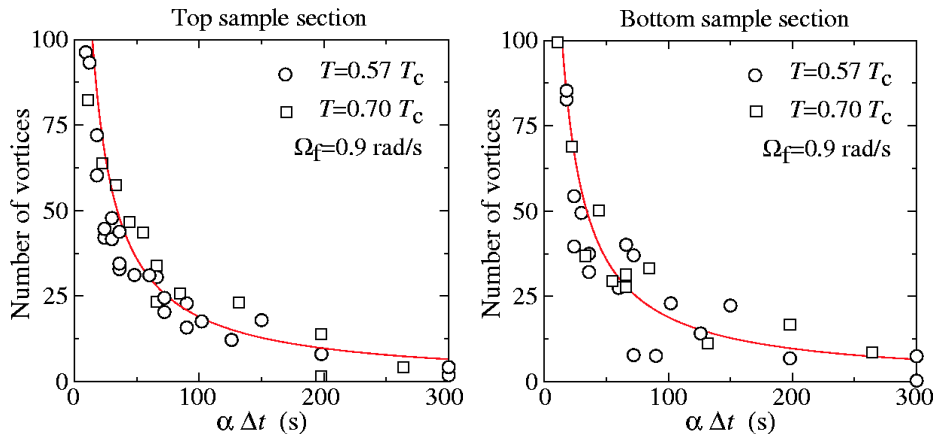


Fig. 3. Number of remnant \mathcal{N} for A-phase separated top and bottom sample sections, as a function of the waiting period Δt at zero rotation. The results can be fit with $\mathcal{N}(\Delta t) \approx 2 \cdot 10^3 / (\alpha \Delta t + b)$ [where Δt is in sec and $b \approx 7$ s allows for the initial remnants after deceleration to zero]. The data are for $\Omega_f = 0.9$ rad/s at $0.57 T_c$ with $\alpha = 0.60$ and at $0.7 T_c$ with $\alpha = 1.1$.

vortices.⁵ This gives N in the final state at Ω_f . At temperatures above the transition to turbulence T_{on} we equate N with the number of remnants \mathcal{N} at the end of the waiting period Δt , while below T_{on} the equilibrium vortex state is created.⁶ In both cases a remnant which starts to evolve has to be above a minimum size which at $\Omega_f = 0.9$ rad/s is $r_o \gtrsim 3 \mu\text{m}$. In comparison, the measured roughness of the quartz surface is typically $\lesssim 1 \mu\text{m}$. The rate of rotation increase $d\Omega/dt$ to the final state Ω_f was found not to influence the results in our operating range $d\Omega/dt \sim 0.001 - 0.04$ rad/s².

Annihilation time of remnants: In Fig. 2 the number of remnants \mathcal{N} is measured at fixed T and Δt as a function of Ω_f . As expected, the results prove to be independent of the choice of Ω_f . The measurement also shows that \mathcal{N} scales with the length of the sample, if $L \gg R$. Thus the annihilation occurs such that the density of remnants decreases roughly at the same rate everywhere along the sample. The configuration before final annihilation is the state of longest life time where only one remnant is present in each cross section of the cylinder. In a long cylinder many remnants can still be stacked after another in configurations like that in Fig. 1.

In Fig. 3 \mathcal{N} has been measured as a function of the waiting period Δt . The monotonic annihilation has been recorded independently for the top and bottom sample sections at two different temperatures. The smooth decay, with $\mathcal{N}(\Delta t) \propto (\alpha \Delta t)^{-1}$, excludes the existence of large numbers of pinned vortices in pinning configurations larger than the equivalent of $r_o \sim 3 \mu\text{m}$. The decay of dynamic remnants is thus governed by Δt and $\alpha(T)$ which

Dynamic remanent vortices in $^3\text{He-B}$

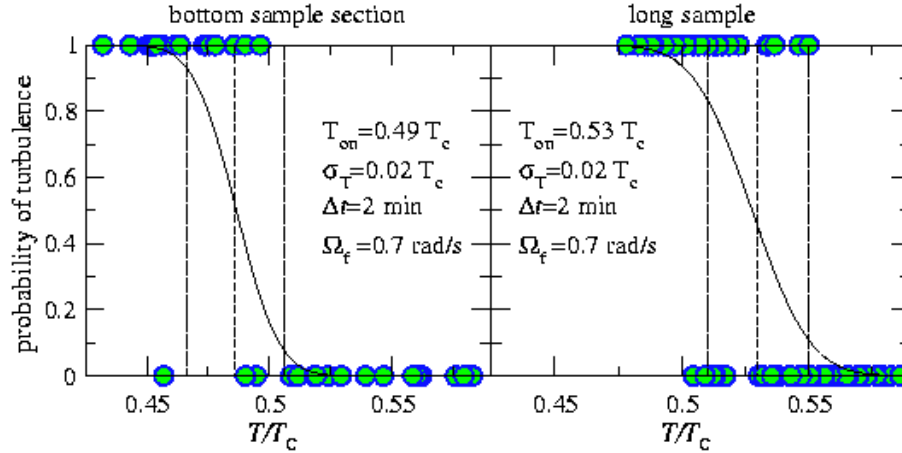


Fig. 4. Onset temperature T_{on} of turbulence, shown here for the A-phase separated bottom section (left) and the long sample with no A phase (right). The probability of turbulence at $\Omega_f = 0.70$ rad/s is plotted as a function of temperature with ~ 40 data points per panel. The A-phase separated top section has an onset distribution with the same half width $\sigma_T = 0.02 T_c$, but centered around $T_{\text{on}} = 0.44 T_c$.

control their number, size, and configuration. To reach vortex-free flow at decreasing temperatures, one has to extend Δt to longer times.

Onset of turbulence: In Fig. 4 the onset temperature T_{on} to turbulence is measured. Each data point is obtained at constant temperature, starting from a state with the remnants after a waiting period of $\Delta t = 2$ min. On the vertical axis we plot the probability of finding the equilibrium vortex state at $\Omega_f = 0.7$ rad/s (with $N_{\text{eq}} \approx 500$ for short sample and 560 for long sample). If this state is observed then the turbulent burst has occurred. In the opposite case only a small number of rectilinear vortices is found ($N \lesssim 35$ in short sample and $\lesssim 55$ in long sample). Such cases where the final number of vortices is clearly between these values are rare and limited to the onset regime around T_{on} . The T_{on} data fit the normal distribution with a half width $\sigma_T \sim 0.02 T_c$.

Compared to the top sample section, the bottom section displays (1) a higher T_{on} and (2) a weaker dependence of T_{on} on Δt and the number of remnants \mathcal{N} . We attribute these differences to the presence of the orifice⁵ on the bottom of the sample cylinder. The lower values of T_{on} in the top section also mean that the AB interface does not promote remanence. In Fig. 4 the bottom section is compared with the long sample, so that in both cases the orifice is present. Since T_{on} is higher for the long cylinder, although the initial density of remnants is the same in the short and long samples (Fig. 2), we conclude that the higher onset arises because there are

twice as many remnants in the long sample and they spend a longer time evolving to rectilinear lines. Thus they have a higher probability to become unstable and generate new vortices during their evolution. At the relatively low dissipation $\alpha(T) \approx 0.4$ in the onset regime the remnants are largely insensitive to the direction of rotation after the waiting period Δt and are easily reoriented when flow is reapplied, even if its direction is opposite from before. In addition to the number of remnants \mathcal{N} (*i.e.* Δt), T_{on} depends also on Ω_f . The different mechanisms are currently under investigation, which influence T_{on} and cause the transition to turbulence.⁷

Consequences: Our results are consistent with the presence of dynamic remnants – no support for pinned remnants is found. In fact, since vortex-free flow down to $0.20 T_c$ is consistently achieved in the present sample cylinder up to velocities of 3 mm/s or more by cooling from high temperatures in rotation, no pinning configurations with $r_o \gtrsim 3 \mu\text{m}$ exist. It thus appears that sufficiently smooth-walled containers exist for $^3\text{He-B}$ in which vortices are not permanently pinned by surface roughness.

To achieve vortex-free rotating flow in an open cylinder non-invasive measurements have to be employed, to avoid internal probes or any components which enhance pinning because of non-uniform geometry. Good control of vortex formation allows studies with new experimental approaches, such as the injection of seed vortices in applied flow. However, with decreasing temperature mutual friction dissipation diminishes and vortex annihilation becomes exceedingly slow. At the lowest temperatures the last dynamic remnants can only be removed by warming up to higher temperatures, to speed up annihilation. Using thermal cycling, relatively high-velocity stable vortex-free flow appears possible even in the zero temperature limit.

In superfluid $^4\text{He-II}$ literature it is usual to assume that remanent vortices originate from surface pinning. Since $\alpha \lesssim 0.1$ in most of the experimental temperature range of $^4\text{He-II}$, dynamic remanence is more prevalent there than in $^3\text{He-B}$. With careful selection and preparation of the container walls one can suppress surface roughness to $\lesssim 1 \mu\text{m}$, so that pinned remnants will remain immobile at $v \lesssim 3 \text{mm/s}$. In this range of applied flow the present considerations about dynamic remnants apply equally to $^4\text{He-II}$.

REFERENCES

1. V.M.H. Ruutu *et al.*, *J. Low Temp. Phys.* **107**, 93 (1997).
2. T.D.C. Bevan *et al.*, *J. Low Temp. Phys.* **109**, 423 (1997).
3. M. Krusius *et al.*, *Phys. Rev.* **B47**, 15113 (1993-II).
4. R. Hänninen, A. Mitani, and M. Tsubota, *J. Low Temp. Phys.*, **138**, 589 (2005).
5. A.P. Finne *et al.*, *J. Low Temp. Phys.* **136**, 249 (2004).
6. A.P. Finne *et al.*, *Phys. Rev. Lett.* **96**, 85301 (2006).
7. A.P. Finne *et al.*, *Rep. Prog. Phys.* **69**, 3157 (2006).